Title	Higher-order multipole amplitude measurement in ψ′→γχc2

Higher-order multipole amplitude measurement in $\psi' \to \gamma\chi_{c2}$

M. Ablikim,[1] M. N. Achasov,[5] D. Alberto,[40] F. F. An,[1] Q. An,[38] Z. H. An,[1] J. Z. Bai,[1] R. Baldini,[19] Y. Ban,[25] J. Becker,[2] N. Berger,[1] M. Bertani,[19] J. M. Bian,[1] E. Boger,[17,*] O. Bondarenko,[18] I. Boyko,[17] R. A. Briere,[3] V. Bytev,[17] X. Cai,[1] A. C. Calcaterra,[19] G. F. Cao,[1] J. F. Chang,[1] G. Chelkov,[17,*] G. Chen,[1] H. S. Chen,[1] J. C. Chen,[1] M. L. Chen,[1] S. J. Chen,[23] Y. Chen,[1] Y. B. Chen,[1] H. P. Cheng,[13] Y. P. Chu,[1] D. Cronin-Hennessy,[37] H. L. Dai,[1] J. P. Dai,[1] D. Dedovich,[17] Z. Y. Deng,[1] I. Denysenko,[17,†] M. Destefanis,[40] Y. Ding,[21] L. Y. Dong,[1] M. Y. Dong,[1] S. X. Du,[43] J. Fang,[1] S. S. Fang,[1] C. Q. Feng,[38] C. D. Fu,[1] J. L. Fu,[23] Y. Gao,[34] C. Geng,[38] K. Goetzen,[7] W. X. Gong,[1] M. Greco,[40] M. H. Gu,[1] Y. T. Gu,[9] Y. H. Guan,[6] A. Q. Guo,[24] L. B. Guo,[22] Y. P. Guo,[24] Y. L. Han,[1] X. Q. Hao,[1] F. A. Harris,[36] K. L. He,[1] M. He,[1] Z. Y. He,[24] Y. K. Heng,[1] Z. L. Hou,[1] H. M. Hu,[1] J. F. Hu,[6] T. Hu,[1] B. Huang,[1] G. M. Huang,[14] J. S. Huang,[11] X. T. Huang,[27] Y. P. Huang,[1] T. Hussain,[39] C. S. Ji,[38] Q. Ji,[1] X. B. Ji,[1] X. L. Ji,[1] L. K. Jia,[1] L. L. Jiang,[1] X. S. Jiang,[1] J. B. Jiao,[27] Z. Jiao,[13] D. P. Jin,[1] S. Jin,[1] F. F. Jing,[34] N. Kalantar-Nayestanaki,[18] M. Kavatsyuk,[18] W. Kuehn,[35] W. Lai,[1] J. S. Lange,[35] J. K. C. Leung,[33] C. H. Li,[1] Cheng Li,[38] Cui Li,[38] D. M. Li,[43] F. Li,[1] G. Li,[1] H. B. Li,[1] J. C. Li,[1] K. Li,[10] Lei Li,[1] N. B. Li,[22] Q. J. Li,[1] S. L. Li,[1] W. D. Li,[1] W. G. Li,[1] X. L. Li,[27] X. N. Li,[1] X. Q. Li,[24] X. R. Li,[26] Z. B. Li,[31] H. Liang,[38] Y. F. Liang,[29] Y. T. Liang,[35] X. T. Liao,[1] B. J. Liu,[32] C. L. Liu,[3] C. X. Liu,[1] C. Y. Liu,[1] F. H. Liu,[28] Fang Liu,[1] Feng Liu,[14] H. Liu,[1] H. B. Liu,[6] H. H. Liu,[12] H. M. Liu,[1] H. W. Liu,[1] J. P. Liu,[41] K. Liu,[25] K. Liu,[6] K. Y. Liu,[21] Q. Liu,[36] S. B. Liu,[38] X. Liu,[20] X. H. Liu,[1] Y. B. Liu,[24] Y. W. Liu,[38] Yong Liu,[1] Z. A. Liu,[1] Zhiqiang Liu,[1] Zhiqing Liu,[1] H. Loehner,[18] G. R. Lu,[11] H. J. Lu,[13] J. G. Lu,[1] Q. W. Lu,[28] X. R. Lu,[6] Y. P. Lu,[1] C. L. Luo,[22] M. X. Luo,[42] T. Luo,[36] X. L. Luo,[1] M. Lv,[1] C. L. Ma,[6] F. C. Ma,[21] H. L. Ma,[1] Q. M. Ma,[1] S. Ma,[1] T. Ma,[1] X. Ma,[1] X. Y. Ma,[1] M. Maggiora,[40] Q. A. Malik,[39] H. Mao,[1] Y. J. Mao,[25] Z. P. Mao,[1] J. G. Messchendorp,[18] J. Min,[1] T. J. Min,[1] R. E. Mitchell,[16] X. H. Mo,[1] N. Yu. Muchnoi,[5] Y. Nefedov,[17] I. B. Nikolaev,[5] Z. Ning,[1] S. L. Olsen,[26] Q. Ouyang,[1] S. Pacetti,[19] J. W. Park,[26] M. Pelizaeus,[36] K. Peters,[7] J. L. Ping,[22] R. G. Ping,[1] R. Poling,[37] C. S. J. Pun,[33] M. Qi,[23] S. Qian,[1] C. F. Qiao,[6] X. S. Qin,[1] J. F. Qiu,[1] K. H. Rashid,[39] G. Rong,[1] X. D. Ruan,[9] A. Sarantsev,[17,‡] J. Schulze,[2] M. Shao,[38] C. P. Shen,[36,§] X. Y. Shen,[1] H. Y. Sheng,[1] M. R. Shepherd,[16] X. Y. Song,[1] S. Spataro,[40] B. Spruck,[35] D. H. Sun,[1] G. X. Sun,[1] J. F. Sun,[11] S. S. Sun,[1] X. D. Sun,[1] Y. J. Sun,[38] Y. Z. Sun,[1] Z. J. Sun,[1] Z. T. Sun,[38] C. J. Tang,[29] X. Tang,[1] H. L. Tian,[1] D. Toth,[37] G. S. Varner,[36] B. Wang,[9] B. Q. Wang,[25] K. Wang,[1] L. L. Wang,[4] L. S. Wang,[1] M. Wang,[27] P. Wang,[1] P. L. Wang,[1] Q. Wang,[1] Q. J. Wang,[1] S. G. Wang,[25] X. L. Wang,[38] Y. D. Wang,[38] Y. F. Wang,[1] Y. Q. Wang,[27] Z. Wang,[1] Z. G. Wang,[1] Z. Y. Wang,[1] D. H. Wei,[8] Q. G. Wen,[38] S. P. Wen,[1] U. Wiedner,[2] L. H. Wu,[1] N. Wu,[1] W. Wu,[21] Z. Wu,[1] Z. J. Xiao,[22] Y. G. Xie,[1] Q. L. Xiu,[1] G. F. Xu,[1] G. M. Xu,[25] H. Xu,[1] Q. J. Xu,[10] X. P. Xu,[30] Y. Xu,[24] Z. R. Xu,[38] Z. Z. Xu,[38] Z. Xue,[1] L. Yan,[38] W. B. Yan,[38] Y. H. Yan,[15] H. X. Yang,[1] T. Yang,[9] Y. Yang,[14] Y. X. Yang,[8] H. Ye,[1] M. Ye,[1] M. H. Ye,[4] B. X. Yu,[1] C. X. Yu,[24] S. P. Yu,[27] C. Z. Yuan,[1] W. L. Yuan,[22] Y. Yuan,[1] A. A. Zafar,[39] A. Zallo,[19] Y. Zeng,[15] B. X. Zhang,[1] B. Y. Zhang,[1] C. Zhang,[23] C. C. Zhang,[1] D. H. Zhang,[1] H. H. Zhang,[31] H. Y. Zhang,[1] J. Zhang,[22] J. Q. Zhang,[1] J. W. Zhang,[1] J. Y. Zhang,[1] J. Z. Zhang,[1] L. Zhang,[23] S. H. Zhang,[1] T. R. Zhang,[22] X. J. Zhang,[1] X. Y. Zhang,[27] Y. Zhang,[1] Y. H. Zhang,[1] Y. S. Zhang,[9] Z. P. Zhang,[38] Z. Y. Zhang,[41] G. Zhao,[1] H. S. Zhao,[1] Jiawei Zhao,[38] Jingwei Zhao,[1] Lei Zhao,[38] Ling Zhao,[1] M. G. Zhao,[24] Q. Zhao,[1] S. J. Zhao,[43] T. C. Zhao,[1] X. H. Zhao,[23] Y. B. Zhao,[1] Z. G. Zhao,[38] Z. L. Zhao,[9] A. Zhemchugov,[17,*] B. Zheng,[1] J. P. Zheng,[1] Y. H. Zheng,[6] Z. P. Zheng,[1] B. Zhong,[1] J. Zhong,[2] L. Zhong,[34] L. Zhou,[1] X. K. Zhou,[6] X. R. Zhou,[38] C. Zhu,[1] K. Zhu,[1] K. J. Zhu,[1] S. H. Zhu,[1] X. L. Zhu,[34] X. W. Zhu,[1] Y. S. Zhu,[1] Z. A. Zhu,[1] J. Zhuang,[1] B. S. Zou,[1] J. H. Zou,[1] and J. X. Zuo[1]

(BESIII Collaboration)

[1]*Institute of High Energy Physics, Beijing 100049, People's Republic of China*
[2]*Bochum Ruhr-University, 44780 Bochum, Germany*
[3]*Carnegie Mellon University, Pittsburgh, Pennsylvania 15213, USA*
[4]*China Center of Advanced Science and Technology, Beijing 100190, People's Republic of China*
[5]*G. I. Budker Institute of Nuclear Physics SB RAS, Novosibirsk 630090, Russia*
[6]*Graduate University of Chinese Academy of Sciences, Beijing 100049, People's Republic of China*
[7]*GSI Helmholtzcentre for Heavy Ion Research GmbH, D-64291 Darmstadt, Germany*
[8]*Guangxi Normal University, Guilin 541004, People's Republic of China*
[9]*Guangxi University, Naning 530004, People's Republic of China*
[10]*Hangzhou Normal University, Hangzhou 310036, People's Republic of China*
[11]*Henan Normal University, Xinxiang 453007, People's Republic of China*
[12]*Henan University of Science and Technology, Luoyang 471003, People's Republic of China*
[13]*Huangshan College, Huangshan 245000, People's Republic of China*

[14]*Huazhong Normal University, Wuhan 430079, People's Republic of China*
[15]*Hunan University, Changsha 410082, People's Republic of China*
[16]*Indiana University, Bloomington, Indiana 47405, USA*
[17]*Joint Institute for Nuclear Research, 141980 Dubna, Russia*
[18]*KVI/University of Groningen, 9747 AA Groningen, The Netherlands*
[19]*Laboratori Nazionali di Frascati—INFN, 00044 Frascati, Italy*
[20]*Lanzhou University, Lanzhou 730000, People's Republic of China*
[21]*Liaoning University, Shenyang 110036, People's Republic of China*
[22]*Nanjing Normal University, Nanjing 210046, People's Republic of China*
[23]*Nanjing University, Nanjing 210093, People's Republic of China*
[24]*Nankai University, Tianjin 300071, People's Republic of China*
[25]*Peking University, Beijing 100871, People's Republic of China*
[26]*Seoul National University, Seoul, 151-747 Korea*
[27]*Shandong University, Jinan 250100, People's Republic of China*
[28]*Shanxi University, Taiyuan 030006, People's Republic of China*
[29]*Sichuan University, Chengdu 610064, People's Republic of China*
[30]*Soochow University, Suzhou 215006, People's Republic of China*
[31]*Sun Yat-Sen University, Guangzhou 510275, People's Republic of China*
[32]*The Chinese University of Hong Kong, Shatin, N.T., Hong Kong*
[33]*The University of Hong Kong, Pokfulam, Hong Kong*
[34]*Tsinghua University, Beijing 100084, People's Republic of China*
[35]*Universitaet Giessen, 35392 Giessen, Germany*
[36]*University of Hawaii, Honolulu, Hawaii 96822, USA*
[37]*University of Minnesota, Minneapolis, Minnesota 55455, USA*
[38]*University of Science and Technology of China, Hefei 230026, People's Republic of China*
[39]*University of the Punjab, Lahore-54590, Pakistan*
[40]*University of Turin and INFN, Turin, Italy*
[41]*Wuhan University, Wuhan 430072, People's Republic of China*
[42]*Zhejiang University, Hangzhou 310027, People's Republic of China*
[43]*Zhengzhou University, Zhengzhou 450001, People's Republic of China*

(Received 9 October 2011; published 22 November 2011)

Using 106×10^6 ψ' events collected with the BESIII detector at the BEPCII storage ring, the higher-order multipole amplitudes in the radiative transition $\psi' \to \gamma\chi_{c2} \to \gamma\pi^+\pi^-/\gamma K^+K^-$ are measured. A fit to the χ_{c2} production and decay angular distributions yields M2 $= 0.046 \pm 0.010 \pm 0.013$ and E3 $= 0.015 \pm 0.008 \pm 0.018$, where the first errors are statistical and the second systematic. Here M2 denotes the normalized magnetic quadrupole amplitude and E3 the normalized electric octupole amplitude. This measurement shows evidence for the existence of the M2 signal with 4.4σ statistical significance and is consistent with the charm quark having no anomalous magnetic moment.

DOI: 10.1103/PhysRevD.84.092006 PACS numbers: 13.20.Gd, 13.25.Gv, 13.40.Hq

I. INTRODUCTION

The radiative transitions $\psi' \to \gamma\chi_{cJ}$ ($J = 1, 2$) provide information about the electromagnetic interaction between charm and anticharm quarks in charmonia and allow the investigation of many interesting topics, including whether the charm quark has an anomalous magnetic moment [1,2] or if there is S-wave and D-wave state mixing [3]. In general, the transition amplitude of radiative decays of charmonium states is dominated by the electric dipole (E1) contribution, with higher multipoles suppressed by powers of photon energy divided by charm quark mass [4]. The search for contributions of higher-order multipole amplitudes is of interest as a source of information on the charm quark's magnetic moment; the possibility of anomalous magnetic moments of heavy quarks being larger than those of lighter ones was raised in Ref. [5]. In $\psi' \to \gamma\chi_{c2}$, taking the charm quark to have a mass $m_c = 1.5$ GeV$/c^2$ and an anomalous magnetic moment κ, M2$=0.029(1+\kappa)$ is predicted [4].

Disagreement between a pure E1 calculation and experimental measurements [6] hints that higher-order multipole amplitudes may exist. These would be reflected in the angular distributions of both the radiative photon and the final state particles [7,8]. Thus, careful investigation of the angular distributions is important.

[*]Also at the Moscow Institute of Physics and Technology, Moscow, Russia.
[†]On leave from the Bogolyubov Institute for Theoretical Physics, Kiev, Ukraine.
[‡]Also at the PNPI, Gatchina, Russia.
[§]Now at Nagoya University, Nagoya, Japan.

TABLE I. Current experimental measurements of the normalized M2 contributions in the decays $\chi_{c1} \to \gamma J/\psi$ and $\psi' \to \gamma\chi_{c1}$.

Experiment	$\chi_{c1} \to \gamma J/\psi$	$\psi' \to \gamma\chi_{c1}$	Signal events
Crystal Ball [9]	$-0.002^{+0.008}_{-0.020}$	$0.077^{+0.050}_{-0.045}$	921
E-835 [10]	$0.002 \pm 0.032 \pm 0.004$	...	2090
CLEO-c [13]	$-0.0626 \pm 0.0063 \pm 0.0024$	$0.0276 \pm 0.0073 \pm 0.0023$	39 363

TABLE II. Current experimental measurements of the normalized M2 contributions in the decays $\chi_{c2} \to \gamma J/\psi$ and $\psi' \to \gamma\chi_{c2}$.

Experiment	$\chi_{c2} \to \gamma J/\psi$	$\psi' \to \gamma\chi_{c2}$	Signal events
Crystal Ball [9]	$-0.333^{+0.116}_{-0.292}$	$0.132^{+0.098}_{-0.075}$	441
E-760 [11]	-0.14 ± 0.06	...	1904
E-835 [10]	$-0.093^{+0.039}_{-0.041} \pm 0.006$	...	5908
BESII [12]	...	$-0.051^{+0.054}_{-0.036}$	731
CLEO-c [13]	$-0.079 \pm 0.019 \pm 0.003$	$0.002 \pm 0.014 \pm 0.004$	19 755

Several experiments, including the Crystal Ball experiment in $\psi' \to \gamma\chi_{c1,c2} \to \gamma\gamma J/\psi \to \gamma\gamma\ell^+\ell^-(\ell = e \text{ or } \mu)$ [9], the E-835 experiment in $p\bar{p} \to \chi_{c1,c2} \to \gamma J/\psi \to \gamma e^+ e^-$ [10], the E-760 experiment in $p\bar{p} \to \chi_{c2} \to \gamma J/\psi \to \gamma e^+ e^-$ [11], and the BESII experiment in $\psi' \to \gamma\chi_{c2} \to \gamma\pi^+\pi^-/\gamma K^+K^-$ [12], have searched for higher-order multipole amplitudes. Because of their limited statistics, they were unable to provide evidence for the existence of higher-order multipoles. More recently, the CLEO experiment reported measurements of higher-order multipole amplitudes in $\psi' \to \gamma\chi_{c1,c2} \to \gamma\gamma J/\psi \to \gamma\gamma\ell^+\ell^-$ [13], where significant M2 contributions were found in the $\psi' \to \gamma\chi_{c1}$ and $\chi_{c1,c2} \to \gamma J/\psi$ transitions. Tables I and II summarize the experimental measurements on searches for higher-order multipole amplitudes.

In this article, $(1.06 \pm 0.04) \times 10^8$ ψ' events [14] accumulated in the BESIII experiment are used in the selection of $\psi' \to \gamma\chi_{c2}$, $\chi_{c2} \to \pi^+\pi^-/K^+K^-$ events, which allow the determination of the higher-order multipole amplitudes in the $\psi' \to \gamma\chi_{c2}$ transition.

II. THE BESIII EXPERIMENT AND DATA SET

This analysis is based on a 156.4 pb^{-1} of ψ' data corresponding to $(1.06 \pm 0.04) \times 10^8$ ψ' events [14] collected with the BESIII detector [15] operating at the BEPCII Collider [16]. In addition, an off-resonance sample of 42.6 pb^{-1} taken at $\sqrt{s} = 3.65$ GeV is used for the study of continuum backgrounds.

BESIII/BEPCII [15] is a major upgrade of the BESII experiment at the BEPC accelerator [16] for studies of hadron spectroscopy and τ-charm physics [17]. The design peak luminosity of the double-ring e^+e^- collider, BEPCII, is 10^{33} cm^{-2} s^{-1} at beam currents of 0.93 A. The BESIII detector with a geometrical acceptance of 93% of 4π consists of the following main components: (1) a small-celled, helium-based main draft chamber with 43 layers, where the average single wire resolution is 135 μm, and the momentum resolution for 1 GeV/c charged particles in a 1 T magnetic field is 0.5%; (2) an electromagnetic calorimeter (EMC) made of 6240 CsI (Tl) crystals arranged in a cylindrical shape (barrel) plus two end caps (for 1.0 GeV photons, the energy resolution is 2.5% in the barrel and 5% in the end caps, and the position resolution is 6 mm in the barrel and 9 mm in the end caps); (3) a time-of-flight system (TOF) for particle identification (PID) composed of a barrel part made of two layers with 88 pieces of 5 cm thick, 2.4 m long plastic scintillators in each layer, and two end caps with 48 fan-shaped, 5 cm thick, plastic scintillators in each end cap (the time resolution is 80 ps in the barrel and 110 ps in the end caps, corresponding to a K/π separation of more than 2σ for momenta below about 1 GeV/c); (4) a muon chamber system made of 1000 m^2 of resistive plate chambers arranged in nine layers in the barrel and eight layers in the end caps and incorporated in the return iron yoke of the superconducting magnet (the position resolution is about 2 cm).

The optimization of the event selection and the estimation of physics backgrounds are performed through Monte Carlo (MC) simulations. The GEANT4-based simulation software BOOST [18] includes the geometric and material description of the BESIII detectors and the detector response and digitization models, as well as the tracking of the detector running conditions and performance. The production of the ψ' resonance is simulated by the MC event generator KKMC [19], while the decays are generated by EVTGEN [20] for known decay modes with branching ratios being set to PDG [21] world average values, and by

LUNDCHARM [22] for the remaining unknown decays. The analysis is performed in the framework of the BESIII offline software system [23] which takes care of the detector calibration, event reconstruction, and data storage.

MC samples of $\psi' \to \gamma\chi_{c0,c2} \to \gamma\pi^+\pi^-/\gamma K^+K^-$ are generated according to phase space to determine the normalization factors in the partial wave analysis [12,24], and MC samples of $\psi' \to (\gamma)e^+e^-/(\gamma)\mu^+\mu^-$ and $\psi' \to XJ/\psi$ ($X = \pi^0\pi^0$, η) with $J/\psi \to (\gamma)\mu^+\mu^-$ are generated for background studies.

III. DATA ANALYSIS

Charged tracks are reconstructed in the main draft chamber, and the number of charged tracks is required to be 2 and have no net charge. For each track, the polar angle must satisfy $|\cos\theta| < 0.93$, and the point of closest approach must be within ± 10 cm of the interaction point in the beam direction and within ± 1 cm of the beam line in the plane perpendicular to the beam. The TOF (both end cap and barrel) and dE/dx measurements for each charged track are used to calculate $\chi^2_{\rm PID}(i)$ values and the corresponding confidence levels ${\rm Prob}_{\rm PID}(i)$ for the hypotheses that a track is a pion, kaon, or proton, where $i(i = \pi/K/p)$ is the particle type. For pion candidates, ${\rm Prob}_{\rm PID}(\pi) > 0.001$ is required, while for kaon candidates, ${\rm Prob}_{\rm PID}(K) > {\rm Prob}_{\rm PID}(\pi)$ and ${\rm Prob}_{\rm PID}(K) > 0.001$ are required.

Electromagnetic showers are reconstructed by clustering EMC crystal energies. The energy deposited in nearby TOF counters is included to improve the reconstruction efficiency and energy resolution. Showers identified as photon candidates must satisfy fiducial and shower-quality requirements. The minimum energy is 25 MeV for barrel showers ($|\cos\theta| < 0.8$) and 50 MeV for end-cap showers ($0.86 < |\cos\theta| < 0.92$). The showers in the angular range between the barrel and end cap are poorly reconstructed and excluded from the analysis. To eliminate showers from charged particles, a photon must be separated by at least 20° from any charged track. EMC cluster timing requirements are used to suppress electronic noise and energy deposits unrelated to the event. The number of good photon candidates is required to be larger than or equal to 1 in each event, and the photon with the highest energy is regarded as the radiative photon from $\psi' \to \gamma\chi_{c2}$.

In order to separate pions and kaons more effectively and to distinguish χ_{c0} and χ_{c2} more clearly, a four-constraint kinematic fit is performed with the two charged tracks and the radiative photon candidate under the hypotheses that the two tracks are either $\pi^+\pi^-$ or K^+K^-, and the kinematic chi-squares, χ^2_π and χ^2_K, are determined. If $\chi^2_\pi < \chi^2_K$ and $\chi^2_\pi < 60$, the event is categorized as $\gamma\pi^+\pi^-$; otherwise, if $\chi^2_K < \chi^2_\pi$ and $\chi^2_K < 60$, the event is categorized as γK^+K^-. For the selected $\gamma\pi^+\pi^-$ and γK^+K^- candidate events, at least one of the charged tracks is required to be identified as a π for $\gamma\pi^+\pi^-$ or a K for γK^+K^-.

To remove $e^+e^- \to (\gamma)e^+e^-$ and $\psi' \to (\gamma)e^+e^-$ backgrounds, the deposited energy of each track in the EMC is required to be less than 1.4 GeV, and the observed ionization is also required to be within 3σ of the expected value for each track. Furthermore, in $\gamma\pi^+\pi^-$, observed ionization of charged tracks is required to be within 2σ of the expected value when the polar angle of the charged track is within the EMC insensitive region (i.e. $0.81 < |\cos\theta| < 0.86$). These requirements remove almost all events with two electron tracks but still keep the efficiencies for the signal channels very high: 96% for $\gamma\pi^+\pi^-$ and 97% for γK^+K^-.

In $\gamma\pi^+\pi^-$, there are $e^+e^- \to (\gamma)\mu^+\mu^-$ and $\psi' \to (\gamma)\mu^+\mu^-$ backgrounds due to π/μ misidentification. In order to remove the backgrounds with $\mu^+\mu^-$, the deposited energy in the EMC of at least one of the charged tracks is required to be larger than 0.34 GeV. Over 99% of the $e^+e^- \to (\gamma)\mu^+\mu^-$ and $\psi' \to (\gamma)\mu^+\mu^-$ backgrounds are removed after applying this requirement. Since μ/K misidentification is quite small, it is not necessary to apply this requirement in the γK^+K^- decay.

After performing all the above selection criteria, clean $\psi' \to \gamma\chi_{c0,c2} \to \gamma\pi^+\pi^-/\gamma K^+K^-$ data samples

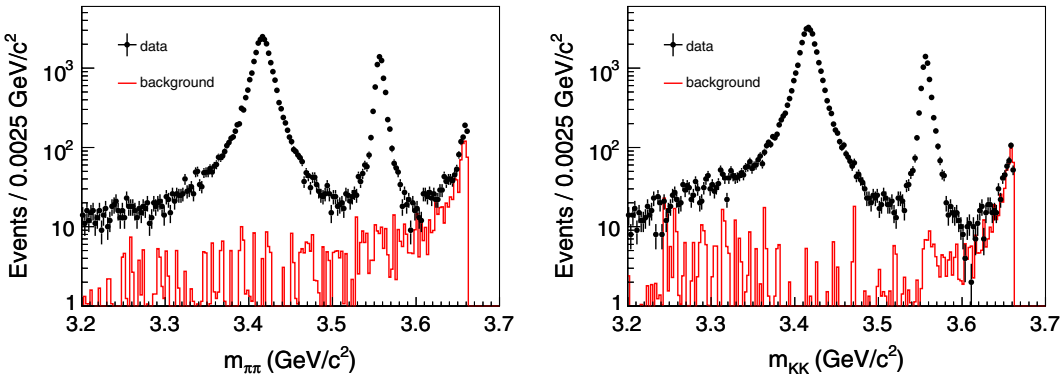

FIG. 1 (color online). The invariant mass distributions of $\pi^+\pi^-$ (left panel) and K^+K^- (right panel) for the selected $\gamma\pi^+\pi^-$ and γK^+K^- events from ψ' data. Dots with error bars are data, while blank histograms are the sum of MC simulated backgrounds and normalized continuum background (estimated from the data sample taken at $\sqrt{s} = 3.65$ GeV).

are obtained. The $\pi^+\pi^-$ and K^+K^- invariant mass distributions are shown in Fig. 1. Clear χ_{c0} and χ_{c2} signals are observed, and the background levels within the χ_{c2} signal region between 3.53 and 3.59 GeV/c^2 are 2.6% [0.7% $\psi' \to (\gamma)\mu^+\mu^-$, 0.8% normalized continuum, 0.3% cross contamination from $\chi_{c2} \to K^+K^-$, 0.7% χ_{c0} tail, and 0.1% $\psi' \to \pi^+\pi^-/\pi^+\pi^-\pi^0$ events] for $\gamma\pi^+\pi^-$ and 2.1% [0.7% cross contamination from $\chi_{c2} \to \pi^+\pi^-$, 1.1% χ_{c0} tail, and 0.3% $\psi' \to K^+K^-$ events] for γK^+K^-. The highest mass peak corresponds to ψ' decays to two charged tracks that are kinematically fitted with an unassociated low energy photon. Requiring the invariant mass of the two charged tracks to be between 3.53 and 3.59 GeV/c^2 to select χ_{c2}, 7154 $\gamma\pi^+\pi^-$ events and 6657 γK^+K^- events are obtained.

IV. FIT TO THE ANGULAR DISTRIBUTIONS

The formulas for the helicity amplitudes in $\psi' \to \gamma\chi_{c2} \to \gamma PP$ ($P = \pi/K$), which include higher-order multipole amplitudes, are widely discussed in Refs. [7,8,12]:

$$\begin{aligned} W(\theta_\gamma, \theta_M, \phi_M) = {} & 3\sin^2\theta_\gamma \sin^2(2\theta_M)x^2 + \frac{3}{2}(1+\cos^2\theta_\gamma)\sin^4\theta_M y^2 - \frac{3}{\sqrt{2}}\sin(2\theta_\gamma)\sin(2\theta_M)\sin^2\theta_M \cos\phi_M xy \\ & + \sqrt{3}\sin(2\theta_\gamma)\sin(2\theta_M)(3\cos^2\theta_M - 1)\cos\phi_M x + \sqrt{6}\sin^2\theta_\gamma \sin^2\theta_M(3\cos^2\theta_M - 1)\cos 2\phi_M y \\ & + (1+\cos^2\theta_\gamma)(3\cos^2\theta_M - 1)^2, \end{aligned} \tag{1}$$

where $x = A_1/A_0$, $y = A_2/A_0$, and $A_{0,1,2}$ are the χ_{c2} helicity 0, 1, 2 amplitudes, respectively. θ_γ is the polar angle of the radiative photon, where the electron beam is defined as the z axis in the e^+e^- center-of-mass frame, and θ_M and ϕ_M are the polar and azimuthal angles of the π/K in the χ_{c2} rest frame, where the polar axis is defined with respect to the radiative photon direction and $\phi_M = 0$ is defined by the electron beam direction.

An unbinned maximum likelihood fit to the joint production and decay angular distribution is performed to determine x and y values. We define six factors [24]:

$$a_1 = 3\sin^2\theta_\gamma \sin^2(2\theta_M), \tag{2}$$

$$a_2 = \tfrac{3}{2}(1+\cos^2\theta_\gamma)\sin^4\theta_M, \tag{3}$$

$$a_3 = -\frac{3}{\sqrt{2}}\sin(2\theta_\gamma)\sin(2\theta_M)\sin^2\theta_M\cos\phi_M, \tag{4}$$

$$a_4 = \sqrt{3}\sin(2\theta_\gamma)\sin(2\theta_M)(3\cos^2\theta_M - 1)\cos\phi_M, \tag{5}$$

$$a_5 = \sqrt{6}\sin^2\theta_\gamma\sin^2\theta_M(3\cos^2\theta_M - 1)\cos 2\phi_M, \tag{6}$$

$$a_6 = (1+\cos^2\theta_\gamma)(3\cos^2\theta_M - 1)^2. \tag{7}$$

The mean values of $a_1, a_2, a_3, a_4, a_5, a_6$ are determined with $\psi' \to \gamma\chi_{c2}$, $\chi_{c2} \to \pi^+\pi^-/K^+K^-$ MC events, where phase space is used for the simulation of all the angular distributions:

$$\bar{a}_n = \frac{\Sigma_{i=1}^N a_n(i)}{N}, \qquad n = 1, \ldots, 6. \tag{8}$$

Here N is the number of events after all selections from phase space MC samples. We integrate first the parts independent of the parameters in the angular distribution to make the fit faster. Since $\bar{a}_n$ is calculated with phase space MC events, it naturally accounts for the detector acceptance effects.

Then, the constructed probability-density function is written as

$$f(x, y) = \frac{W(\theta_\gamma, \theta_M, \phi_M)}{\bar{a}_1 x^2 + \bar{a}_2 y^2 + \bar{a}_3 xy + \bar{a}_4 x + \bar{a}_5 y + \bar{a}_6}. \tag{9}$$

In practice, we use the log-likelihood function, which is given by $\ln\mathcal{L} = \Sigma_{i=1}^N \ln f_i(x, y)$, for convenience, where the sum is over the events in the signal region. The dominant background events are simulated by MC events, and their normalized contributions are subtracted in $\ln\mathcal{L}$ value, i.e. $\ln\mathcal{L}_s = \ln\mathcal{L} - \ln\mathcal{L}_b$, where $\ln\mathcal{L}_b$ is the normalized sum of logarithmic likelihood values from background events.

Before fitting to the data, input and output checks have been done using MC samples, and the checked results verify the validity of the fitting procedure. An unbinned maximum likelihood fit to the $\gamma\pi^+\pi^-$ and γK^+K^- production and decay angular distributions yields

$$x_\pi = 1.55^{+0.08}_{-0.07}, \qquad y_\pi = 2.06^{+0.10}_{-0.09}, \qquad \rho_\pi = 0.890, \tag{10}$$

$$x_K = 1.55 \pm 0.08, \qquad y_K = 2.13^{+0.11}_{-0.10}, \qquad \rho_K = 0.902, \tag{11}$$

where the errors are statistical, and ρ_π, ρ_K are the correlation coefficients between x and y for $\gamma\pi^+\pi^-$ and γK^+K^-, respectively. A simultaneous fit to $\gamma\pi^+\pi^-$ and γK^+K^- gives

$$x = 1.55 \pm 0.05, \qquad y = 2.10 \pm 0.07, \qquad \rho = 0.896, \tag{12}$$

where errors are statistical, and ρ is the correlation coefficient between x and y. The normalized M2 and E3 amplitudes are calculated to be [1]

$$\mathrm{M2} = 0.046 \pm 0.010, \qquad \mathrm{E3} = 0.015 \pm 0.008 \tag{13}$$

based on the simultaneous fit result, where errors are statistical only. Figure 2 shows the angular distributions

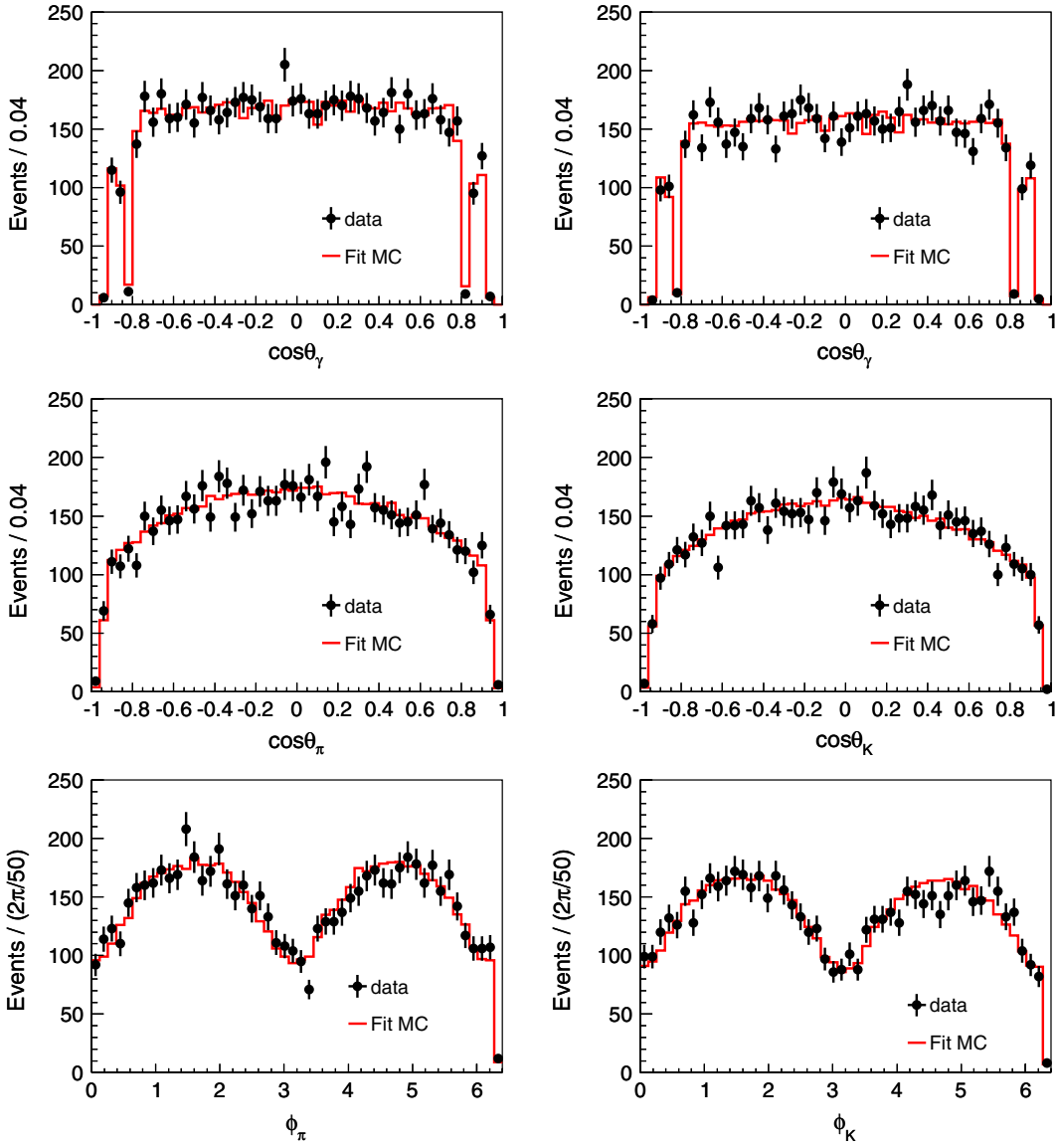

FIG. 2 (color online). The angular distributions of $\cos\theta_\gamma$, $\cos\theta_M$, and ϕ_M for $\chi_{c2} \to \pi^+\pi^-$ (left panel) and $\chi_{c2} \to K^+K^-$ (right panel), where the dots with error bars are data and the histograms are the fitted results.

of data and the fitted results for both $\gamma\pi^+\pi^-$ and γK^+K^- events. Good agreement is observed for all angular distributions.

The goodness of the fit is estimated using Pearson's χ^2 test [25]. The data sample is divided into $8 \times 8 \times 8 = 512$ bins in $\cos\theta_\gamma$, $\cos\theta_M$, and ϕ_M, and the χ^2 value is calculated as

$$\chi^2 = \sum_i \frac{(n_i^{DT} - n_i^{\rm MC})^2}{n_i^{DT}}, \qquad (14)$$

where n_i^{DT} and $n_i^{\rm MC}$ are the number of observed events in the ith bin from data and the corresponding number of normalized events from MC using x and y fixed to the values determined in the analysis. Here MC events are 20 times more than data events. For bins with less than seven events, we add the events into the adjacent bin. The result yields $\chi^2_\pi/\text{n.d.f.} = 377.5/368 = 1.03$ for $\gamma\pi^+\pi^-$ and $\chi^2_K/\text{n.d.f.} = 348.1/354 = 0.98$ for γK^+K^-, where n.d.f. is the number of degrees of freedom. These results show that the fits are good.

V. SYSTEMATIC ERRORS

A. MC simulation of detector response

The consistency between data and MC simulation for χ_{c2} events can be tested using χ_{c0} events. The angular distribution of χ_{c0} is unambiguous, i.e., $W_0 = 1 + \cos^2\theta_\gamma$. If we replace the $(3\cos^2\theta_M - 1)^2$ term in Eq. (1) by 1, then Eq. (1) becomes equal to W_0 when both x and y equal zero. Therefore, if we fit the angular distribution of χ_{c0} events with a modified Eq. (1) using the same method as in χ_{c2}

decays, $x = 0$ and $y = 0$ are expected. Nonzero x and y values from the fit reflect the difference between data and MC and give a measure of the systematic error due to the MC simulation of the detector response. The fitted results are $x_\pi = 0.049^{+0.016}_{-0.017}$, $y_\pi = -(0.024 \pm 0.011)$, $\rho_\pi = 0.037$ for $\gamma\pi^+\pi^-$, $x_K = 0.073 \pm 0.015$, $y_K = 0.004 \pm 0.010$, $\rho_K = 0.077$ for γK^+K^-, and $x = 0.062 \pm 0.011$, $y = -(0.008 \pm 0.007)$, $\rho = 0.058$ for the simultaneous fit. The systematic error is taken as the shift from 0 plus its error. Assuming the correlation factor is 1 between x and y for the central value, 0.06, 0.04, and -0.63 are obtained for Δx_π, Δy_π, and $\rho_\pi^{\rm sys}$, respectively; 0.08, 0.02, and 0.52 are obtained for Δx_K, Δy_K, and $\rho_K^{\rm sys}$, respectively; and for the simultaneous fit, 0.07, 0.02, and -0.43 are obtained for Δx, Δy, and $\rho^{\rm sys}$, respectively. Studies with the MC demonstrate that a systematic error in modeling the θ_γ, ϕ_M, or θ_M efficiency produces a shift of x and y of approximately the same size in both χ_{c0} and χ_{c2} samples, where the latter sample is generated with our nominal results for x and y. Therefore, we assume the observed shift from $x = 0$ and $y = 0$ for the true χ_{c0} data is an estimate of the systematic error on the measured values of x and y for radiative decays to χ_{c2}.

The systematic error of the detector response contains systematic errors associated with the simulation of charged track finding, photon detection efficiency, mass resolution of χ_{c2}, kinematic fit, PID efficiency, trigger efficiency, etc. Comparisons between data and MC simulation for the angular distributions of χ_{c0} decay events are shown in Fig. 3.

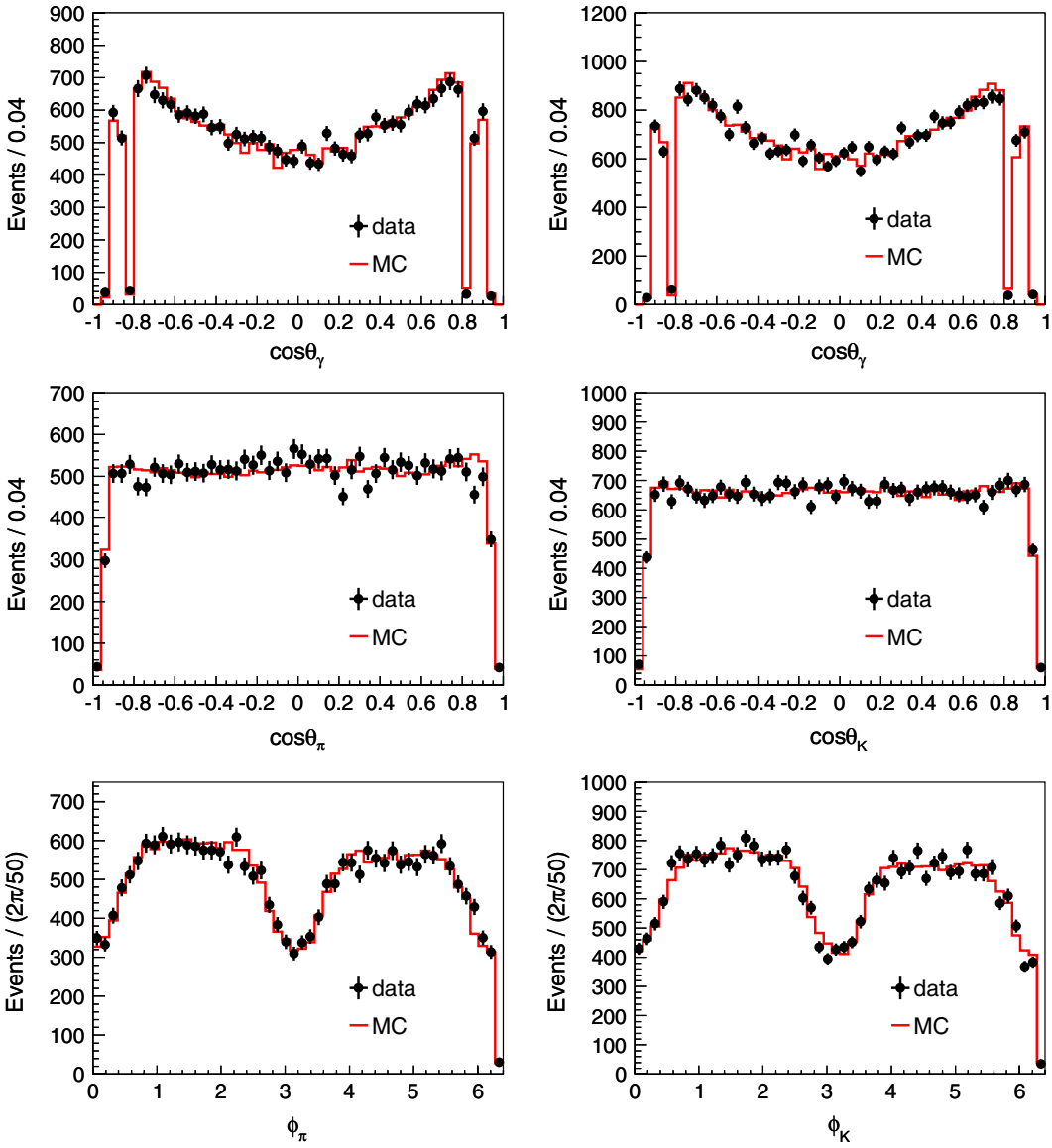

FIG. 3 (color online). Comparisons of $\cos\theta_\gamma$, $\cos\theta_M$, and ϕ_M angular distributions between data (dots with error bars) and MC simulation (histograms) for $\chi_{c0} \to \pi^+\pi^-$ (left panel) and $\chi_{c0} \to K^+K^-$ (right panel).

B. $\mu^+\mu^-$ background in $\gamma\pi^+\pi^-$

In $\gamma\pi^+\pi^-$, the dominant backgrounds are $(\gamma)\mu^+\mu^-$ events and continuum events, which contribute at the 1.5% level. The $\psi' \to (\gamma)\mu^+\mu^-$ background events are estimated by MC simulation, while the continuum events are estimated using the data sample taken at $\sqrt{s} = 3.65$ GeV. The μ/π misidentification ratio has been checked using a control sample of $\psi' \to \pi^+\pi^- J/\psi \to \pi^+\pi^-\mu^+\mu^-$, and its value is measured to be $(1.7 \pm 2.6)\%$. Considering the uncertainty from the $\psi' \to \mu^+\mu^-$ branching ratio (10.4%) [21], the $(\gamma)\mu^+\mu^-$ background level is determined to be $(1.5 \pm 0.2)\%$. We vary the background level by 1σ (from 1.5% to 1.7% or 1.3%) in the fit and take the difference of the fitted x and y values as the systematic error due to the $\mu^+\mu^-$ background uncertainty. The differences are $\Delta x = 0.02$, $\Delta y = 0.03$.

C. $\gamma\pi^+\pi^-$ and γK^+K^- cross contamination

The systematic error arising from $\gamma\pi^+\pi^-$ and γK^+K^- cross contamination is also determined by MC simulation. The γK^+K^- background contamination in $\gamma\pi^+\pi^-$ is 0.3%, while the $\gamma\pi^+\pi^-$ background contamination in γK^+K^- is 0.7%. Signal MC samples of $\gamma\pi^+\pi^-$ and γK^+K^- with $x = \sqrt{3}$, $y = \sqrt{6}$ are generated and mixed according to the estimated amount of cross contamination determined by MC simulation. The differences on the fitted x and y values are taken as the systematic errors due to the $\gamma\pi^+\pi^-$ and γK^+K^- cross contamination, which are $\Delta x_\pi = 0.01$, $\Delta y_\pi = 0.02$ for $\gamma\pi^+\pi^-$ and $\Delta x_K = 0.01$, $\Delta y_K = 0.02$ for γK^+K^-.

D. χ_{c0} contamination

There are some χ_{c0} events in the χ_{c2} signal region due to the overlap of the $\pi^+\pi^-/K^+K^-$ invariant mass peaks. The contamination from $\chi_{c0} \to \pi^+\pi^-$ background events is only about 0.7% for $\chi_{c2} \to \pi^+\pi^-$, and the contamination from $\chi_{c0} \to K^+K^-$ background events is 1.1% for $\chi_{c2} \to K^+K^-$ according to MC simulations. Signal MC samples of $\chi_{c0} \to \pi^+\pi^-/K^+K^-$ are generated and mixed into $\chi_{c2} \to \pi^+\pi^-/K^+K^-$ signal MC samples according to the estimated contamination ratio determined by MC simulation. The differences on the fitted x and y values from the input ones are taken as the systematic errors. The systematic uncertainties due to χ_{c0} contamination can be ignored for $\chi_{c2} \to \pi^+\pi^-$, while they are $\Delta x_K = 0.01$, $\Delta y_K = 0.02$ for $\chi_{c2} \to K^+K^-$.

E. Total systematic error

The systematic error sources discussed above are summarized in Table III. Here the correlation coefficients (ρ_π and ρ_K) from background uncertainties, including $\mu^+\mu^-$ background, π/K cross contamination background, and χ_{c0} background contamination, are set to 1, and the total correlation coefficient ρ is calculated as $\rho = \sum_i \frac{\rho_i \sigma_{xi} \sigma_{yi}}{\sigma_x \sigma_y}$, where i runs over all systematic errors. The total systematic errors are $\Delta x_\pi = 0.07$, $\Delta y_\pi = 0.06$ in $\gamma\pi^+\pi^-$, $\Delta x_K = 0.08$, $\Delta y_K = 0.04$ in γK^+K^-, and $\Delta x = 0.07$, $\Delta y = 0.05$ in the simultaneous fit.

VI. CONCLUSION AND DISCUSSION

The final helicity amplitude results are

$$x_\pi = 1.55^{+0.08}_{-0.07} \pm 0.07, \quad y_\pi = 2.06^{+0.10}_{-0.09} \pm 0.06, \quad \rho_\pi^{\rm stat} = 0.890, \quad \rho_\pi^{\rm sys} = -0.17 \tag{15}$$

for $\gamma\pi^+\pi^-$,

$$x_K = 1.55 \pm 0.08 \pm 0.08, \quad y_K = 2.13^{+0.11}_{-0.10} \pm 0.04, \quad \rho_K^{\rm stat} = 0.902, \quad \rho_K^{\rm sys} = 0.38 \tag{16}$$

for γK^+K^-, and

$$x = 1.55 \pm 0.05 \pm 0.07, \quad y = 2.10 \pm 0.07 \pm 0.05, \quad \rho^{\rm stat} = 0.896, \quad \rho^{\rm sys} = 0.26 \tag{17}$$

for the simultaneous fit, where the first errors are statistical and the second systematic. $\rho^{\rm stat}$ and $\rho^{\rm sys}$ are the correlation coefficients between x and y of the statistical and systematic errors. Then the normalized M2 and E3 amplitudes are determined to be

$$\begin{aligned} {\rm M2} &= 0.046 \pm 0.010 \pm 0.013, \\ {\rm E3} &= 0.015 \pm 0.008 \pm 0.018, \end{aligned} \tag{18}$$

where the first errors are statistical and the second systematic. By investigating the difference of the logarithmic likelihoods between a pure E1 transition and the best nominal fit, the statistical significance of the M2 amplitude contribution is estimated to be 4.4σ, which means

TABLE III. Summary of the systematic errors and correlations.

Source	x_π	y_π	ρ_π	x_K	y_K	ρ_K
MC simulation	0.06	0.04	−0.63	0.08	0.02	0.52
$\mu^+\mu^-$ background	0.02	0.03	1	⋯	⋯	⋯
π/K cross contamination	0.01	0.02	1	0.01	0.02	1
χ_{c0} contamination	⋯	⋯	⋯	0.01	0.02	1
Total	0.07	0.06	−0.17	0.08	0.04	0.38

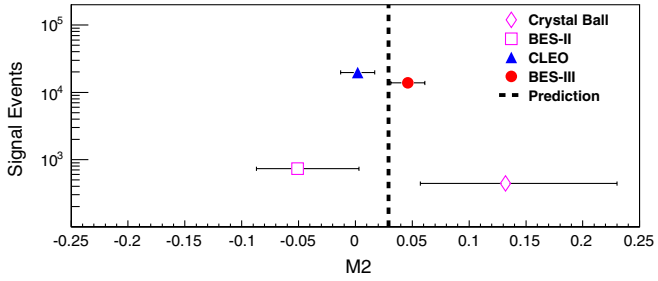

FIG. 4 (color online). Experimental measurements for the normalized M2 amplitude together with the theoretical prediction [1,2], assuming the charm quark mass to be 1.5 GeV/c^2 and no anomalous magnetic moment. CLEO's result is from a free E3 amplitude fit.

evidence of the M2 contribution has been observed. As for the E3 signal, the current measurement is consistent with zero. The M2 experimental results from different measurements are shown in Fig. 4. Our measurement agrees with predictions and is consistent with CLEO's result within 2σ when E3 is free [13] and BESII's result [12] within 1.7σ.

In summary, the higher-order multipole amplitudes in $\psi' \to \gamma\chi_{c2} \to \gamma\pi^+\pi^-/\gamma K^+K^-$ are studied with the BESIII experiment based on $(1.06 \pm 0.04) \times 10^8$ ψ' events. Evidence of an M2 amplitude is observed. This measurement agrees with predictions and is consistent with the charm quark having no anomalous magnetic moment [1,2,4].

ACKNOWLEDGMENTS

The BESIII Collaboration thanks the staff of BEPCII and the computing center for their hard efforts. This work is supported in part by the Ministry of Science and Technology of China under Contract No. 2009CB825200; National Natural Science Foundation of China under Contracts No. 10625524, No. 10821063, No. 10825524, No. 10835001, and No. 10935007; the Chinese Academy of Sciences (CAS) Large-Scale Scientific Facility Program; CAS under Contracts No. KJCX2-YW-N29 and No. KJCX2-YW-N45; 100 Talents Program of CAS; Istituto Nazionale di Fisica Nucleare, Italy; the Siberian Branch of the Russian Academy of Science, Joint Project No. 32 with CAS; U. S. Department of Energy under Contracts No. DE-FG02-04ER41291, No. DE-FG02-91ER40682, and No. DE-FG02-94ER40823; University of Groningen and the Helmholtzzentrum fuer Schwerionenforschung GmbH, Darmstadt; and the WCU Program of the National Research Foundation of Korea under Contract No. R32-2008-000-10155-0.

[1] J. L. Rosner, Phys. Rev. D **78**, 114011 (2008).
[2] K. J. Sebastian, H. Grotch, and F. L. Ridener, Phys. Rev. D **45**, 3163 (1992).
[3] P. Moxhay and J. L. Rosner, Phys. Rev. D **28**, 1132 (1983).
[4] G. Karl, S. Meshkov, and J. L. Rosner, Phys. Rev. Lett. **45**, 215 (1980); V. A. Novikov *et al.*, Phys. Rep. **41**, 1 (1978).
[5] D. A. Geffen and W. Wilson, Phys. Rev. Lett. **44**, 370 (1980).
[6] E. Eichten *et al.*, Phys. Rev. D **21**, 203 (1980).
[7] P. K. Kabir and A. J. G. Hey, Phys. Rev. D **13**, 3161 (1976).
[8] C. Edwards *et al.*, Phys. Rev. D **25**, 3065 (1982).
[9] M. Oreglia *et al.* (Crystal Ball Collaboration), Phys. Rev. D **25**, 2259 (1982).
[10] M. Ambrogiani *et al.* (E835 Collaboration), Phys. Rev. D **65**, 052002 (2002).
[11] T. Armstrong *et al.* (E760 Collaboration), Phys. Rev. D **48**, 3037 (1993).
[12] M. Ablikim *et al.* (BES Collaboration), Phys. Rev. D **70**, 092004 (2004).
[13] M. Artuso *et al.* (CLEO Collaboration), Phys. Rev. D **80**, 112003 (2009).
[14] M. Ablikim *et al.* (BESIII Collaboration), Phys. Rev. D **81**, 052005 (2010).
[15] M. Ablikim *et al.* (BESIII Collaboration), Nucl. Instrum. Methods Phys. Res., Sect. A **614**, 345 (2010).
[16] J. Z. Bai *et al.* (BES Collaboration), Nucl. Instrum. Methods Phys. Res., Sect. A **344**, 319 (1994); **458**, 627 (2001).
[17] D. M. Asner *et al.*, Int. J. Mod. Phys. A **24**, 499 (2009).
[18] Z. Y. Deng *et al.*, High Energy Phys. Nucl. Phys. **30**, 371 (2006).
[19] S. Jadach, B. F. L. Ward, and Z. Was, Comput. Phys. Commun. **130**, 260 (2000); Phys. Rev. D **63**, 113009 (2001).
[20] R. G. Ping *et al.*, Chinese Phys. C **32**, 599 (2008).
[21] K. Nakamura *et al.* (Particle Data Group), J. Phys. G **37**, 075021 (2010).
[22] J. C. Chen, G. S. Huang, X. R. Qi, D. H. Zhang, and Y. S. Zhu, Phys. Rev. D **62**, 034003 (2000).
[23] W. D. Li, H. M. Liu *et al.*, in *Proceeding of CHEP06, Mumbai, India, 2006*, edited by Sunanda Banerjee (Tata Institute of Fundamental Research, Mumbai, 2006).
[24] Xin Shi, Master thesis, Peking University, 2004.
[25] W. Eadie *et al.*, *Statistical Methods in Experimental Physics* (North-Holland Publishing Company, Amsterdam-London, 1971).